

PCCP

Accepted Manuscript



This is an *Accepted Manuscript*, which has been through the Royal Society of Chemistry peer review process and has been accepted for publication.

Accepted Manuscripts are published online shortly after acceptance, before technical editing, formatting and proof reading. Using this free service, authors can make their results available to the community, in citable form, before we publish the edited article. We will replace this *Accepted Manuscript* with the edited and formatted *Advance Article* as soon as it is available.

You can find more information about *Accepted Manuscripts* in the [Information for Authors](#).

Please note that technical editing may introduce minor changes to the text and/or graphics, which may alter content. The journal's standard [Terms & Conditions](#) and the [Ethical guidelines](#) still apply. In no event shall the Royal Society of Chemistry be held responsible for any errors or omissions in this *Accepted Manuscript* or any consequences arising from the use of any information it contains.



Journal Name

ARTICLE

Specific effects in microwave chemistry explored through reactor vessel design, theory, and spectroscopy

Bridgett Ashley^{a,b}, Derek D. Lovingood^c, Yu-Che Chiu^d, Hanwei Gao^d, Jeffery Owens^b, Geoffrey F. Strouse^{a,†}

Received 00th January 20xx,
Accepted 00th January 20xx

DOI: 10.1039/x0xx00000x

www.rsc.org/

Abstract: Microwave chemistry has revolutionized synthetic methodology for the preparation of organics, pharmaceuticals, materials, and peptides. The enhanced reaction rates commonly observed in a microwave have led to wide speculation about the function of molecular microwave absorption and whether the absorption leads to microwave specific effects and enhanced molecular heating. The comparison of theoretical modeling, reactor vessel design, and dielectric spectroscopy allows the nuance of the interaction to be directly understood. The study clearly shows an unaltered silicon carbide vessel allows measurable microwave penetration and therefore, molecular absorption of the microwave photons by the reactants within the reaction vessel cannot be ignored when discussing the role of molecular heating in enhanced molecular reactivity for microwave synthesis. The results of the study yield an improved microwave reactor vessel design that eliminates microwave leakage into the reaction volume by incorporating a noble metal surface layer onto a silicon carbide reaction vessel. The systematic study provides the necessary theory and measurements to better inform the arguments in the field.

Much of the excitement of microwave (MW) chemistry revolves around the concept that uniform, rapid volumetric heating is achieved within the reaction vessel as it is irradiated, thus leading to highly efficient product formation by overcoming kinetic and thermodynamic barriers through the addition of external energy. The high efficiency of MW heating has led to the use of MW reactors to improve the carbon footprint in chemistry or, in effect, the “greenness” of preparing desired molecules, a grand challenge in synthetic chemistry. The energy efficiency of conversion of MW photons into heat has been theorized to lower energy consumption by 72%, compared to traditional thermal reactions.^[1–5]

In response, a rapid growth of publications utilizing MW chemistry has occurred in the literature, including nanoscience organs, following our report on MW-initiated nucleation of reactants leading to uniform nanocrystal growth with greatly shortened reaction times.^[6–7] Why such drastic MW enhancement is observed in the reaction rate is widely debated and, in the case of nanomaterials, the role of MW photon absorption by the precursors has been suggested.^[8–12] In MW-enhanced nanomaterial reactions, the resultant controlled growth is more likely due to selective dielectric absorption driving nucleation by conversion of MW into thermal energy by Debye processes, as currently discussed in the literature,^[13, 14] than to non-thermal effects.^[15, 16]

To date, MW synthesis studies show that a MW photon’s energy is too low to break a chemical bond and spectroscopically excites only molecular rotations.^[17] Enhanced heating can occur due to MW-selective interactions with a susceptor,^[18] solvent, polar molecule, or magnetic molecule, or to the influence of reduced thermal gradients and wall effects.^[19–23] Lack of understanding of the involvement of MW absorption and of its influence on MW heating obscures direct comparison of results from nominally identical reactions between researchers, due to small changes in the reaction system.^[24–26] For instance, the use of different reaction conditions (pressure, temperature, time), solvents that absorb MW to various extents, different MW cavity designs, different MW energies, and reactor vessels made of different materials (quartz, glass, silicon carbide [SiC]) has complicated the discussion of MW enhancement of rates of reaction. Stiegman attempted to clarify the question by reaction design,^[27–29] and de la Hoz approached the question by modeling MW interaction.^[25, 30] Leadbeater measured the ability of molecules to thermalize in a solvent bath following MW photon absorption, and concluded that MW absorption leads to rapid thermal diffusion rather than directly enhancing a reaction path.^[31] Kappe approached the discussion by attempting to eliminate solvent and chemical reactant MW absorption by vessel design using a SiC reaction vessel, concluding that MW heating and rapid thermal heating produce the same results in the reactions examined.^[32, 33] To fully understand the impact of MW electromagnetic radiation (EMR) on the rates of reactions, one must consider the interaction of EMR with the vessel and the MW cavity, and MW absorption (imaginary dielectric contribution) versus reflectivity (real dielectric contribution as a total system).

In this report, the interaction of the MW field with the reaction system is explored by theoretical modeling and application of dielectric spectroscopy to design a reactor vessel that blocks MW penetration through the vessel walls and thus eliminates MW absorption by the reactants. The design of the MW vessel coupled to

^a Department of Chemistry and Biochemistry, Florida State University, Tallahassee, FL 32306-4390

^b Air Force Civil Engineer Center, Tyndall Air Force Base, FL 32403

^c Universal Technology Corporation, 139 Barnes Dr. Suite 2 Tyndall AFB, FL 32403

^d Department of Physics, Florida State University, Tallahassee, FL 32306

[†] Corresponding author email strouse@chem.fsu.edu

Supporting Information. Electrodynamics simulations via COMSOL for acetonitrile and ethanol (SF1-3), experimental heating curves (SF4-11, 14,15), VNA data for Ag plated vessels (SF 12,13), and COMSOL design (SF16). This material is available free of charge via the Internet at <http://>
See DOI: 10.1039/x0xx00000x

the experimental results will help the researcher better elucidate MW absorption from non-thermal MW interactions across this synthetic field. Among other things these results demonstrate that there is significant MW penetration through the walls of commercial SiC composite MW vessels and that it can be eliminated by noble metal plating of the SiC reactor vessel's interior. The high conductivity of noble metals allows them to reflect the majority of MW radiation away, and to rapidly disperse via ohmic losses the small amount transmitted in a thin layer just a few micrometers thick.

Multiple methods of testing MW leakage into the reaction vessels were used. Modeling the electromagnetic field, measuring the complex permittivity, and correlating heating rates of MW-absorbing molecules were accomplished and confirmed by dielectric spectroscopy and reactant heating experiments. The theoretical and experimental data support the MW engineering predictions that the interaction of MWs with the total reaction system is highly dependent on the reaction system makeup, and involves complex interactions between the interfaces. The experimental evidence for MW transparency of standard MW reactor vessels compared to the SiC-noble metal vessel herein described is shown by comparing the resonant frequency shift for solvents and small-molecule MW susceptors in a MW-transparent solvent. As anticipated from earlier findings,^[6] the addition of a MW-absorbing molecule (tri-*n*-octylphosphine telluride, TOP-Te) into a MW-transparent solvent (toluene) resulted in a linear increase in heating rate at fixed MW power as the concentration of the MW-absorbing molecule was increased. MW absorption by TOP-Te was confirmed by measuring the dielectric shift with increasing TOP-Te concentration. The increased reaction temperature should not be confused with MW-selective bond activation, as the absorption of MW radiation leads to thermal heating of the surrounding solvent bath by phonon coupling.^[34, 35] Researchers have often missed this nuance, which has led to questionable conclusions with respect to the contribution of the MW field to the reaction.^[20, 32] Although partially correct, these conclusions do not properly describe the reaction system.

In today's highly populated, resource-limited world, the development of low-cost energy-efficient synthetic methods is imperative.^[36, 37] The study provide an improved platform for MW syntheses, and clearly demonstrate that system design is critical to reaction analysis. The elimination of EMR leakage by vessel designs that attenuate 100% of the impingent MW radiation will allow researchers to better interrogate the complex reaction landscape in MW chemistry. The results of this study are validated in an Anton-Parr resonant cavity MW reactor, but are applicable to all commercial MW reactor systems that utilize resonant cavities regardless of brand. The understanding of MW heating phenomena and their impact is not limited to chemical reactions, as it is also important in describing electromagnetic interference (EMI) screening, telecommunications, and how radar is scattered by a material. Whether the goal is to prepare phosphors for new solid-state lighting or new catalysts, to deposit organic material for fabric coatings, or to develop novel EMI shielding technologies for the aerospace and telecommunications communities, advances in the field can be achieved only if the microwave interactions can be properly understood under the reaction conditions, and extrapolated to new ones.

EXPERIMENTAL

Materials. Ethylene glycol (Sigma-Aldrich), ethanol (Fisher), acetonitrile (Fisher), and toluene (Fisher) were used without further

purification. Concentrated nitric acid (70%) (Sigma-Aldrich), concentrated hydrochloric acid (37%) (Sigma-Aldrich), hydrogen peroxide (30%) (Sigma-Aldrich), potassium hydroxide (Sigma-Aldrich), silver nitrate (VWR), dextrose (Sigma-Aldrich) (3-aminopropyl)triethoxysilane (Sigma-Aldrich), ammonium hydroxide (Sigma-Aldrich), tri-*n*-octylphosphine (TOP, 90%)(Sigma-Aldrich), and tellurium metal ingots (99.999%) (Sigma-Aldrich) were used without further purification.

Microwave Cross-section. The TOP-Te MW cross section ($\tan \delta$) values were measured at 2.45 GHz using a coaxial transmission line and MuEpsl software from Damaskos on a vector network analyzer (VNA) (Anritsu Lightning 37347E). The real (ϵ') and imaginary (ϵ'') values for the samples were calculated using the Nicholson-Ross-Weir algorithm.^[38] Solvent MW cross sections were taken from literature.

Microwave Field Perturbation. The perturbation of the MW field by the reaction system, which includes the reactor vessel, the solvent, and solute, was analyzed by the frequency shift of the S_{11} standing wave reflection generated using the VNA coupled to a TE_{103} (Transverse Electric mode) resonant cavity tuned to resonate at 2.45025 GHz. The frequency shift and broadening of the S_{11} reflection (Table 2) correlate to the magnitude of ϵ' and ϵ'' , respectively.

Microwave Heating. MW heating was measured for 30 s in an Anton Paar Monowave 300 unit operating in a single-mode (TE_{10x}) self-tuning cavity^[39] at 300 W (constant power) for standard solvents (toluene, acetonitrile, ethanol, and EG) with known $\tan \delta$ and specific heat capacities (C_p). The MW heating experiments were carried out on 3 mL of solvent in 10-mL reaction vessels composed of SiC, borosilicate (BS), SiC with an inner silver coating (Ag/SiC) (in Supporting Information, SF 6), or SiC with an inner gold coating (Au/SiC). The metal coatings were 7 μm Ag and 10 μm Au, respectively. Coating of the SiC and BS vessels is described in the following paragraph. The vessels were sealed under ambient conditions, heated for 30 s at 300 W of continuous power with stirring (600 RPM) while the temperature was simultaneously recorded externally via an infrared sensor and internally using a ruby thermometer. The experiments were carried out under continuous power to eliminate any confounding effects of power oscillations due to differences in various materials' rates of absorption. The maximum observed temperature (pressure) for SiC was 130 °C (10 bar) and for BS 200 °C (10 bar).

Internal Metal coating of microwave reaction vials. The inside of the reaction vessel was silver plated by Tollens' reagent^[40] or electroplated with gold (Component Surfaces, Inc.). Metal coating of the SiC vessel required more aggressive pretreatment of the vessel to ensure a uniform coating of the metal film. The SiC vial was cleaned with concentrated nitric acid (30 min), treated with a solution of H_2O_2 , HCl, and DI water (1:1:5 v:v:v) for 10 min at 80 °C, and washed with DI water between steps. The cleaned SiC vial was dried under a stream of nitrogen, followed by oxygen plasma etching (100% O_2 atm., 30 W; Herrick Plasma Cleaner PDC-001) for 1 min. For silver coating, the SiC vial was activated by exposure to a solution of (3-aminopropyl)triethoxysilane (ATPES) and toluene (volumetric ratio 1:49) for 24 h, rinsed with toluene, and dried following literature protocol.^[41] Approximately ten layers of Ag were deposited in sequential plating reactions carried out by addition of Tollens' reagent in the presence of 5 mM dextrose for 10 min. The Ag/SiC vessels were rinsed three times with DI water and finally with methanol. Fresh Tollens' reagent was prepared by mixing 12 mM

KOH, 3 mM AgNO₃, and excess concentrated NH₃. Gold coating on the SiC was electroplated commercially by Component Surfaces, Inc.

Preparation of n-Trioctylphosphine-Telluride. A 2 M solution of TOP-Te was prepared by combining 10 mL of TOP and 255.2 mg of tellurium ingots in a vial under nitrogen and sonicating the mixture overnight until the tellurium had dissolved to produce a clear, yellow-green solution.

Modeling Field Distribution. The MW electric field and its absorption by various materials were simulated by COMSOL Multiphysics based on finite-element methods. To reduce the complexity of the system without losing the general applicability of the simulation, a 2D waveguide was modeled. The dimensions of 114.41 mm in length and 72.136 mm in height were chosen to match a WR-284 waveguide. The simulated waveguide consisted of top and bottom aluminum walls. Additionally, the left wall was assigned as the activation port through which the 2.45-GHz TE₁₀ mode waveguide was excited; the right wall was designated as a transmitting port, avoiding back reflection and interference in the simulation region. In the simulation with gold coating, the interfaces between the gold with the SiC walls and with the solvent were designated as transition boundaries. These transition boundaries used the appropriate physical parameters of gold.

Results and Discussion

Microwave interactions with the reaction system. Designing a reactor vessel for a MW-assisted synthesis, and understanding the observed impact of the vessel design on the rate of reaction requires a proper description of the impinging EMR MW field on the reaction system's components. In MW chemistry, the absorbed MW photon is converted into thermal energy by coupling with the environment through molecular friction and ionic conduction, and by ohmic (electron polarization), Maxwell-Wagner (charge oscillation) and magnetic processes.^[42] For a typical MW chemical reaction in liquid phase, ionic conduction and molecular friction are the predominant terms leading to heat generation following MW absorption. While MW irradiation can lead to molecular polarization without heat, the heating of a MW synthetic reaction is due to absorption of the MW photon and scattering behavior of the molecules in the reaction mixture. The interaction of the impinging MW field on any material is described in terms of the material's complex dielectric ($\epsilon^* = \epsilon' - i\epsilon''$). The real component ϵ' is the scattering term, describing the ability of the material to reflect or store an electric field. The imaginary term (ϵ'') describes the absorption of the impinging photon, which is converted into heat through molecular motion and solvent thermalization. In effect, this can be thought of as analogous to a Beer-Lambert law problem in absorption spectroscopy. Each constituent of the reaction system will have unique ϵ' and ϵ'' values, which are often reported in terms of the ratio of the dielectric components, known as $\tan \delta$.

$$\tan \delta = \frac{\epsilon''}{\epsilon'} \quad (1)$$

All materials have a MW cross section that can be described in terms of the decrease of EMR power to a value of $1/e$ over a defined material thickness, called the penetration depth (D_p). The value of D_p is dependent on $\tan \delta$ and λ_0 , the frequency of the impinging EMR field:

$$D_p = \frac{\lambda_0}{2\pi(2\epsilon')^{1/2}} \left[(1 + \tan \delta)^{1/2} - 1 \right]^{-1/2} \quad (2)$$

The effect on MW penetration will be influenced by the presence of an interfacial layer and requires the inclusion of the appropriate terms for that interface. An interface comprised of a highly conductive metal will reflect most of an impinging EMR field, and rapidly absorb the small amount of EMR transmitted via ohmic losses. The more conductive the metal, the thinner this absorptive layer needs to be to block MW radiation. The thickness of the layer needed to reduce the EMR field to $1/e$ of its original amplitude is known as the skin depth, δ_s . δ_s is analogous to the D_p but for amplitude rather than power, and is generally used only in reference to metals. As expected, it takes five δ_s to shield against >99% of the EMR field.^[42]

$$\delta_s = (2/\sigma\omega\mu)^{1/2} \quad (3)$$

where σ is the conductivity, ω is the frequency of the EMR and μ is the permeability of the metal (1 for most metals).

Noble metals are known conductors with silver being the largest but also likely to participate in chemical reactions. Gold, while less conductive, is generally considered non-reactive. For the studies, both surfaces were analyzed, but the majority of the studies focus on gold to minimize chemical reactivity concerns and allow adaptation for chemical reaction studies by the MW chemistry community. Using Eqn. 3, a layer of gold 8 μm thick is needed to effectively block 2.45 GHz radiation, while a layer of 7 μm thick of silver would be required. Conductivity of a metal decreases with increasing temperature, and the thickness of the layer needed to block >99% of the MW radiation at 200 °C – the temperature cut off point used in these experiments – can be calculated with Eqn. 4.

$$\rho_T = \rho_0[1 + \alpha(T - T_0)] \quad (4)$$

where ρ_0 is the resistivity of the metal at 20 °C and α is the temperature coefficient. Table 1 lists these for gold and silver. At 200 °C, 8 μm of silver or 10 μm of gold is necessary. Data for the Ag/SiC tube is available in the Supporting Information.

For the studies carried out in an Anton-Parr resonant cavity the experimental studies were conducted on 10 μm of gold plating in

Table 1. Microwave and thermal constants for the reaction system.

MATERIAL	ϵ'	ϵ''	$\tan \delta$	D_p @ 2.45 GHz (mm)	ρ @ 20 °C ($\mu\Omega \cdot$ cm)	α (K^{-1})	Density (g/mL)	Heat Capacity (J/mL·K)	Thermal Conductivity (W/cm·K)	Thermal Diffusivity (cm^2/s)
SiC	9.57 ^[32]	1.56 ^[32]	0.164 ^[32]	38.6*	---	---	---	---	---	---
Borosilicate	4.82 ^[46]	0.026 ^[46]	0.0054 ^[46]	1637.8*	---	---	---	---	---	---
Silver	---	---	---	---	1.59 ^[48]	0.0038 ^[48]	---	---	---	---
Gold	---	---	---	---	2.44 ^[48]	0.0034 ^[48]	---	---	---	---
TOP-Te	2.63 [†]	0.23 [†]	0.088*	136.2*	---	---	~0.831 ^[48]	---	---	---
Toluene	2.4 ^[47]	0.096 ^[47]	0.040 ^[47]	313.4*	---	---	0.8669 ^[48]	1.466 ^[48]	0.00151 ^[48]	0.00103*
Acetonitrile	37.5 ^[47]	2.325 ^[47]	0.062 ^[47]	52.9*	---	---	0.786 ^[48]	1.756 ^[48]	0.00188 ^[48]	0.00107*
Ethanol	24.3 ^[47]	22.866 ^[47]	0.941 ^[47]	4.8*	---	---	0.789 ^[48]	1.918 ^[48]	0.00171 ^[48]	0.00089*
Ethylene Glycol	37.0 ^[47]	49.950 ^[47]	1.350 ^[47]	2.7*	---	---	1.1132 ^[48]	2.681 ^[48]	0.00256 ^[48]	0.00095*

*Calculated, †measured

order to block >99% of the 2.45 GHz radiation up to reaction temperatures of 200 °C. If systems that work at another commonly used industrial MW frequency – 0.92 GHz – are used or if the reaction temperatures are expected to exceed 200 °C, thicker layers of metal will be needed. For example, many nanoparticle reactions are performed at 300 °C or higher. If an industrial or laboratory MW operating at 0.92 GHz was used for this type of reaction, an 18 μ m thick layer of gold is needed to block MW radiation. If, instead, a MW using 5.8 GHz radiation is used for such a reaction, only 7 μ m of gold is needed. It is additionally important to remember that for very powerful industrial systems, which can easily use 24 kW or more, 1% of the radiation may still be a significant amount, and thicker plating would be needed.

The ability of the system to interact with the MW field is material specific and will scale with $\tan \delta$. In Table 1, $\tan \delta$ and D_p values for selected solvents and a common molecular precursor used in nanoparticle synthesis is listed, along with $\tan \delta$ values for SiC and BS, two common MW reaction vessels. The respective $\tan \delta$ of the vessel, solvent and molecular precursors must be considered individually and collectively, as the heating will be the sum of not only the MW absorption and scattering, but also thermal conductivity and convection of the reaction system. Due consideration of all of these components is required to adequately describe the thermal energy conversion processes leading to product formation in MW-assisted reactions.^[42] The conversion of MW absorption (ϵ') into molecular heating is described in terms of the Debye relaxation arising from molecular motion. According to quantum mechanics, molecules can absorb only an entire photon,^[43] so there is a greater statistical probability that a molecule of higher $\tan \delta$ will absorb a given photon, as demonstrated in earlier MW engineering literature.^[44] Therefore, during a MW reaction, selective heating in the reaction system occurs due to disproportionate heating of one molecule over another in accordance with the magnitudes of the respective $\tan \delta$ values and the volume fraction of the molecules in the MW field. In the absence of a strong MW interaction with either the vessel or the solvent, the molecular reactants will interact with the MW photon.

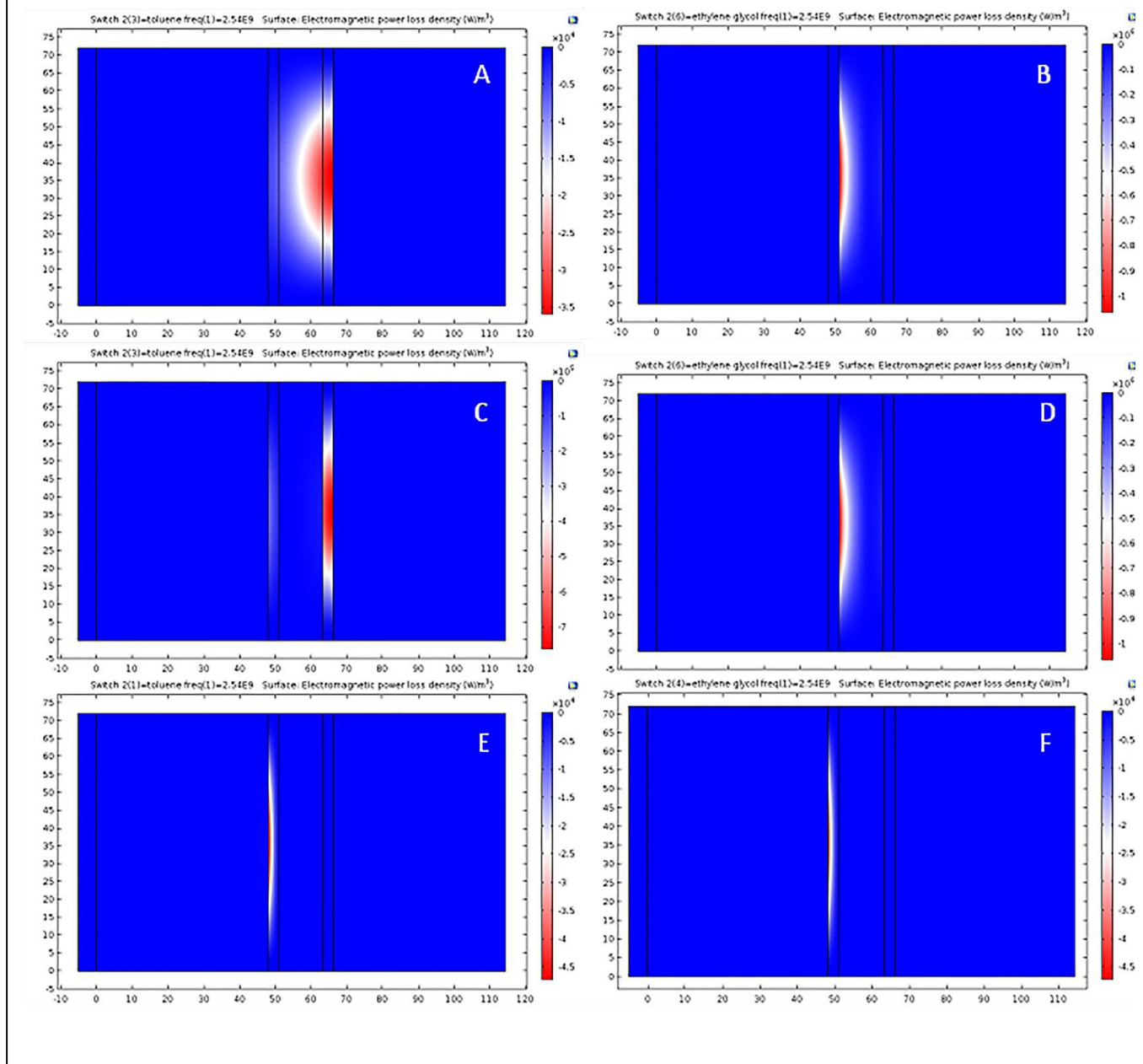
As evidenced in Table 1, the magnitude of contribution is dependent on wall thickness of the vessel and, in a standard MW reactor vessel

(3-mm wall thickness), the MW can interact with the solvent and reactants in the system, as well as with the reactor vessel. The $\tan \delta$ values in Table 1 indicate that synthetic reactions carried out in BS with EG as the solvent will predominately heat by MW absorption of the EG. Likewise, because both BS and toluene have a small $\tan \delta$ and a large D_p , reactions carried out in toluene in a BS reaction vessel will be dominantly heated by the reactants dissolved in toluene. When the BS vessel is replaced by SiC, the magnitudes of $\tan \delta$ and D_p predict competitive MW absorption by the vessel and the reactants. To accurately predict the magnitude of interaction and thus the effect of the complex dielectric to heating in the MW, an electrodynamic (ED) simulation of the total reaction system must be carried out.

Figure 1 shows an ED simulation modeling MW field penetration into a reaction vessel operating in a 2.45-GHz alternating MW field within the cavity of a TE₀₁ waveguide for a series of solvent and reaction vessel configurations containing toluene and EG. The ED simulations for acetonitrile and ethanol are reported in Supporting Information (SF 1–3). A graph of the EM power loss density (EM loss) for all solvents is plotted in Figure 2. For simplicity, the modeling assumes a 2D boundary condition operated in a single-pass configuration to calculate the MW photon absorption by the total reaction system in the MW reactor cavity used in this study. To simulate the reaction vessel, the 3-mm BS, SiC, or Au/SiC walls with a 12-mm inner diameter are modeled as two 3-mm straight walls placed in the middle of the waveguide and separated by the 12-mm solvent volume. The Au/SiC simulation incorporates a 10- μ m layer on the inner walls.

The ED simulation confirms the prediction from Table 1 that the BS walls have the largest EM penetration, whereas the walls of the Au/SiC vessel effectively attenuate EM penetration. For the unaltered SiC vessel the situation is more complicated. For a SiC vessel containing toluene, SiC wall absorption is the major

Figure 1: COMSOL Simulations of TE₀₁ cavity, excited at 2.45 GHz. A (toluene) and B (EG) are of a BS tube placed in the cavity, C (toluene) and D (EG) are of a SiC tube placed in the cavity, and E (toluene) and F (EG) are of a gold plated SiC tube placed in the cavity. Images show the electric field loss vs. distance.

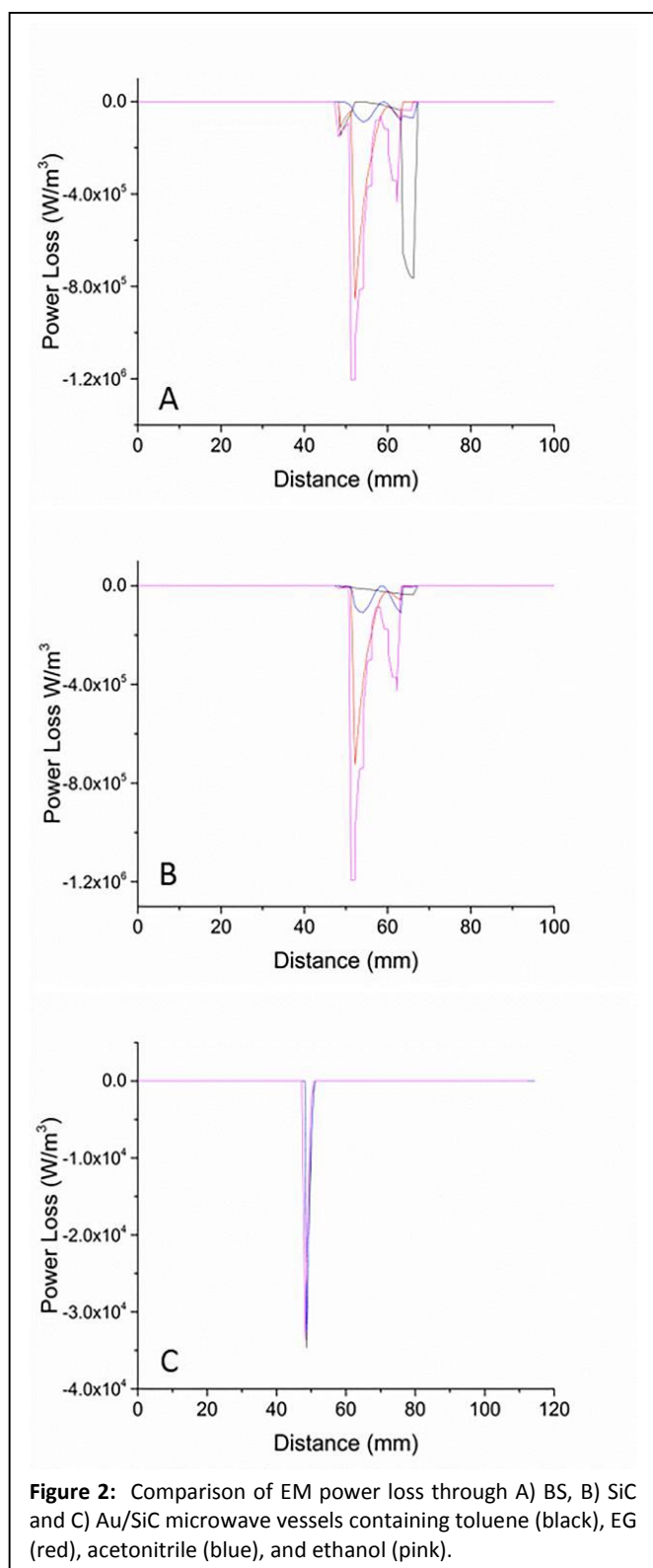


contributor to EM loss (Figure 1C), but in a SiC vessel containing EG, the solvent is the predominant EM loss component (Figure 1D). The contrast between those two can be seen in the line-scan plot (Figure 2). This observation in the ED simulation is easily understood by considering the differences in imaginary permittivity ϵ'' for each component, such that the higher value leads to the larger MW loss component to the ED simulated spectra.

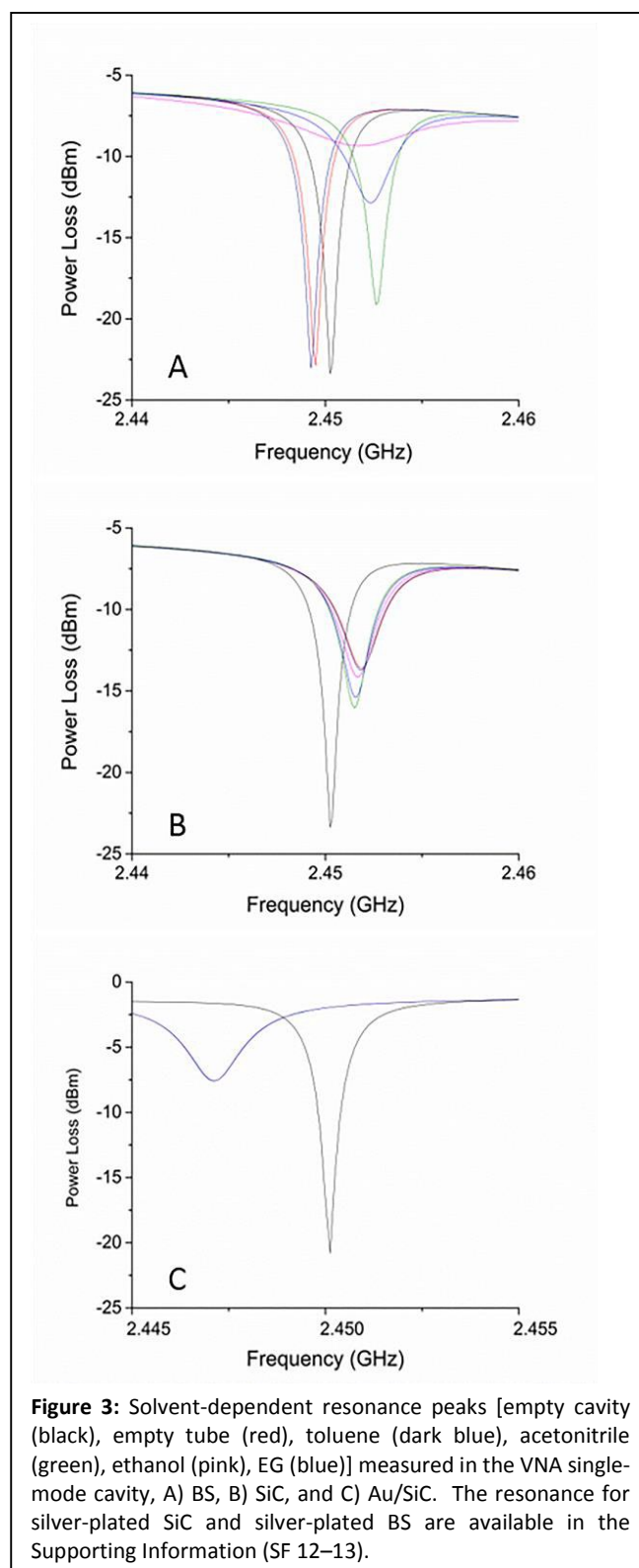
The incorporation of a 10- μm noble metal film at the internal wall surface of the reaction vessel eliminates MW penetration into the reaction volume; thus EM loss can be observed only in the left wall and not in the solvent or right wall. The simulation illustrates that, although $\tan \delta$ is larger for SiC than for BS, the large D_p value leads to a condition wherein the 3-mm wall thickness only partially shields

the contents from the impinging MW photons. The result is that MW leakage into the inner volume of a SiC vessel is $\sim 52\%$ of the original MW photon flux. By contrast, BS allows $\sim 62\%$ of the impinging MW field to pass. Incorporation of the noble metal layer on the inside of the SiC vessel reduces the EMR penetration to $< 1\%$.

The ED simulation predictions can be verified by measuring the MW interaction for the various solvent, molecular precursor, and vessel combinations using a VNA with a resonant cavity. In Figure 3, resonance shift in the VNA cavity is shown for BS, SiC, and Au/SiC reaction vessels containing solvents of different $\tan \delta$. Resonance shifts in Ag/BS and Ag/SiC are available in supporting information (SF 12–13). The VNA measurements represent a qualitative treatment of Slater's perturbation theory to analyze the MW interaction with



the system. The shift in peak resonance frequency reflects the weighted average ϵ' contribution, and changes in full width at half-maximum (FWHM) correspond to ϵ'' .^[49] Shifts from the 2.45025-GHz resonant frequency of the empty TE₁₀₃ resonant cavity measured for air, ethanol, EG, acetonitrile, and toluene in each reaction vessel (BS, SiC, and Au/SiC) are tabulated in Table 2. The change in FWHM of the filled reaction vessel from the empty-cavity resonance is also tabulated.



As predicted from the ED simulations, the frequency shift and FWHM (Figure 3) are more pronounced in the BS vessel than for identical conditions in the SiC, and there is no observable shift for the Au/SiC reactor vessel. The solvent VNA results demonstrate that MW leakage is occurring into the SiC vessel, which is inconsistent with

Table 2: Frequency shifts from 2.45025 GHz and FWHM measurements for reaction vessel and solvent configurations.

	BS	Toluene in BS	Acetonitrile in BS	Ethanol in BS	EG in BS
Frequency Shift (GHz)	-0.0007	-0.001	0.006	0.0015	0.002
FWHM (GHz)	.00875	0.00875	0.00125	0.00575	0.00225
	SiC	Toluene in SiC	Acetonitrile in SiC	Ethanol in SiC	EG in SiC
Frequency Shift (GHz)	0.01625	0.01625	0.00125	0.001375	0.00125
FWHM (GHz)	0.002	0.002	0.0015	0.003	0.0015
	Au/SiC	Toluene in Au/SiC	Acetonitrile in Au/SiC	Ethanol in Au/SiC	EG in Au/SiC
Frequency Shift (GHz)	-0.002875	-0.002875	-0.002875	-0.002875	-0.002875
FWHM (GHz)	0.027	0.027	0.027	0.027	0.027
	BS	mM TOP-Te in Toluene in BS			
		0	0.41	2.06	4.12
Frequency Shift (GHz)	-0.000875	-0.001	-0.001	-0.001	-0.001
FWHM (GHz)	0.00025	0.000375	0.000375	0.0005	0.000625
	SiC	mM TOP-Te in Toluene in SiC			
		0	0.41	2.06	4.12
Frequency Shift (GHz)	-0.001875	-0.001875	-0.001875	-0.001875	-0.001875
FWHM (GHz)	0.001125	0.00125	0.00125	0.00125	0.001375
	Au/SiC	mM TOP-Te in Toluene in Au/SiC			
		0	0.41	2.06	4.12
Frequency Shift (GHz)	-0.002875	-0.002875	-0.002875	-0.002875	-0.002875
FWHM (GHz)	0.027	0.027	0.027	0.027	0.027

previous reported claims.^[33, 50] Evidence of the leakage is quantifiable by inspection of the resonance shift for BS vs. SiC, which shows that the resonant frequency shifts as solvent polarity increases. If the MW field were absorbed only in the SiC walls, then no resonance shift would be observed.

Penetration of the MW field into the interior of the SiC vessel is easily confirmed by measuring the concentration-dependent shift in frequency for a highly polarizable solute in a non-polar solvent. In Figure 4, the concentration-dependent frequency shifts of TOP-Te in toluene are shown in BS, SiC, and Au/SiC. The experimental data reveal a definitive resonance shift with increasing concentration of TOP-Te for BS and SiC, but no shift in the Au/SiC vessel. The observed shift is consistent with theoretical treatment of EM fields in the MW engineering literature,^[45, 49] and confirms the MW photons penetrate standard SiC and BS vessels

MW vessel transparency effects on reaction heating rates. The potential impact of MW on a chemical reaction in a given vessel configuration is most easily understood by comparing the MW heating rates from RT to 100 °C for the non-polar and polar solvents in the BS, SiC, and Au/SiC plated reactor vessels under otherwise

identical conditions. To ensure the heating rate was comparable across systems, the experiment was carried out by employing a 30-s pulse at 300 W and comparing the internal temperature measured by a ruby thermometer to the external temperature reported by the IR thermometer. The upper pressure limit of the reaction vessel was maintained at 10 bar for all solvents, and an upper temperature limit of 200 °C was set to minimize the effect of changes in $\tan \delta$ with temperature.^[51, 52]

In Figure 5, heating curves obtained from the internal ruby thermometer are plotted for each solvent in BS, SiC, and Au/SiC vessels. The heating curve measured by the IR thermometers (external) is available in Supporting Information (SF 4–7). The measured thermal lag (ΔT_r) and the heating rates (dT/dt) are presented in Table 3. In BS the thermal lag is the same across all solvents; the rate of heating scales with the solvent $\tan \delta$ and is impacted to a lesser degree by thermal diffusivity (Figure 5A). For Au/SiC (Figure 5C), ΔT_r and dT/dt are both solvent dependent, and scale with the solvents' thermal diffusivities and not with $\tan \delta$. The behavior for Au/SiC is consistent with predictions for a MW-opaque reaction vessel design. The SiC vessel (Figure 5B) is intermediate

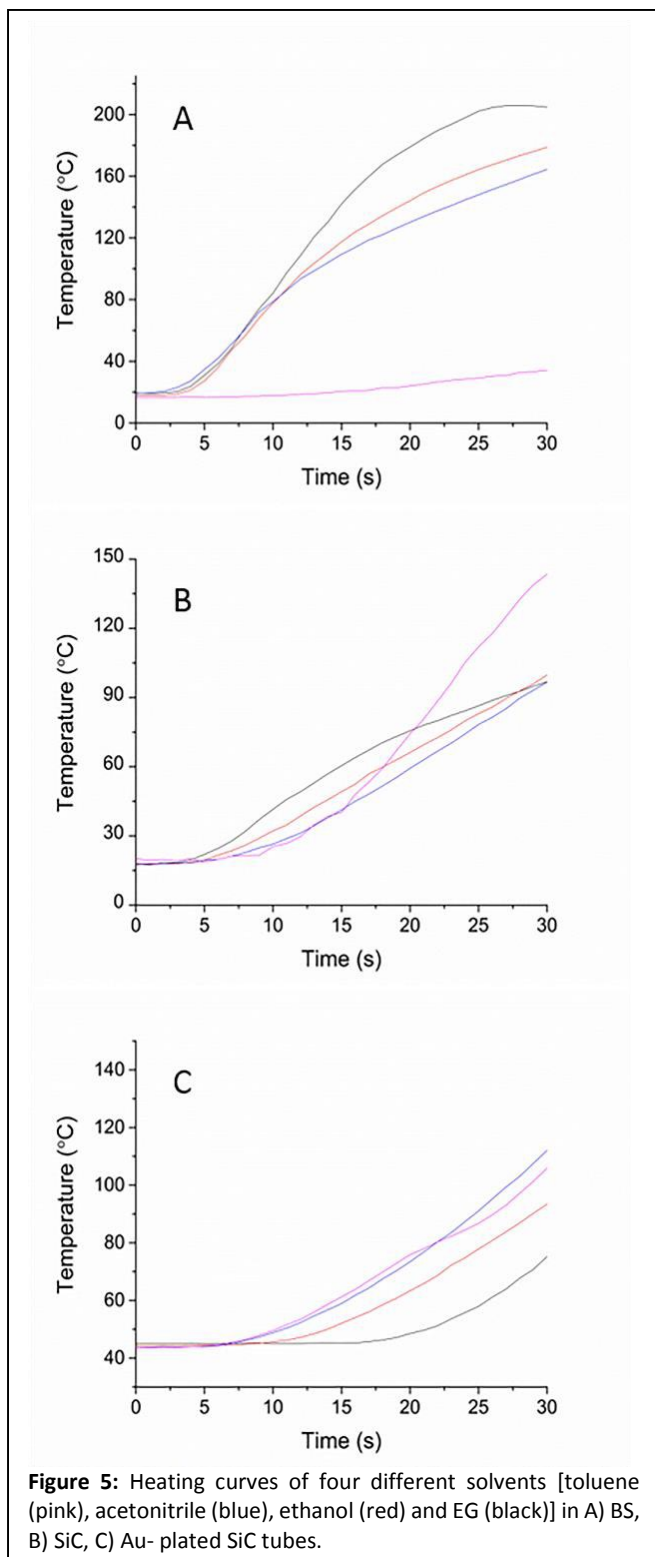


Figure 5: Heating curves of four different solvents [toluene (pink), acetonitrile (blue), ethanol (red) and EG (black)] in A) BS, B) SiC, C) Au-plated SiC tubes.

between the two extremes and the influence of SiC's $\tan \delta$ is clearly discernable. Whereas it is clear that MW absorption into the solvent raises the reaction temperature, thus increasing reaction rate, it is not clear that a molecular reactant can play a significant role via irradiation in a non-absorbing solvent at concentrations used for the nucleation of a nanocrystal.

Recent manuscripts by de la Hoz suggests that materials that absorb MW radiation in a non-polar solvent can enhance reaction rates by transferring energy into the reaction solvent.^[22, 30] To test the

potential for MW-driven nucleation arising from the interaction of a MW photon with the molecular reactant, the heating behavior and VNA results for TOP-Te were analyzed. TOP-Te is reported to be an effective MW absorber for initiating CdTe nanocrystal nucleation in the MW reactor.^[6, 7] The rate of heating for the TOP-Te solution is influenced by $\tan \delta$ and the thermal diffusivity of both solvent and vessel. If a vessel absorbs the preponderance of energy then the temperature is expected to lag between internal and external temperatures, and more importantly to be independent of the solvent's $\tan \delta$, and vice versa. Plots of dT/dt for 0 mM to 4.12 mM TOP-Te in toluene in BS, SiC, and Au/SiC vessels are shown in Figure 6. The heating curves are available in Supporting Information (SF 8–10).

The effect of MW absorption into TOP-Te dissolved in a low- $\tan \delta$ solvent can be understood within the context of the Debye theory, which predicts a linear dependence of $\tan \delta$ based on the molar ratios of solute to solvent, as shown in Eqn. 5

$$\tan \delta(\omega) = C_0 \frac{(\epsilon' + 2)}{\epsilon' k_b T} \mu^2 \frac{\omega \tau_{\text{mean}}}{1 + (\omega \tau_{\text{mean}})^2} \quad (5)$$

where C_0 is a constant dependent on the molar ratios, ϵ' is the real dielectric of the solvent, and μ and τ are the dipole moment and the relaxation time of the solute. The MW absorption cross section is correlated with $\tan \delta$ and thus solvent heating rate by Eqn. 6

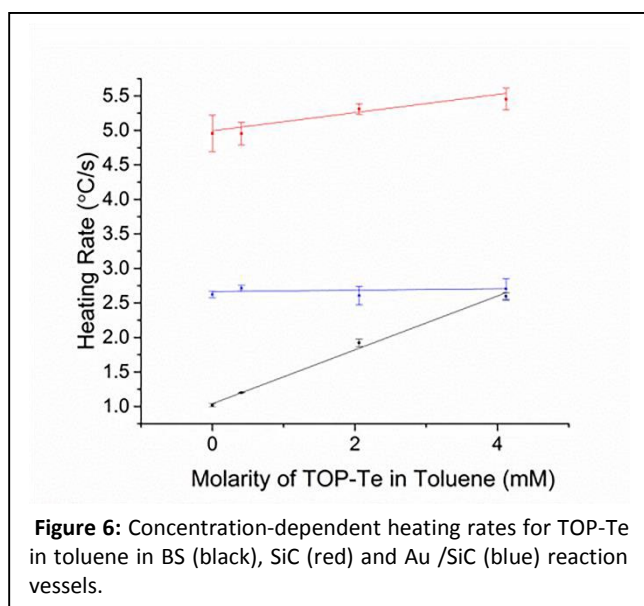
$$P_{\text{abs}} = MC_p \frac{(T - T_0)}{t} = 0.556 \times 10^{-10} \nu \epsilon' * \tan \delta * E_{\text{rms}}^2 V \quad (6)$$

where C_p of a solution is a weighted average of the specific heat capacity of the solvent and solute. At parts per thousand of TOP-Te in toluene, the specific heat capacity can be assumed to be unchanged from that of toluene. Thus the change in heating rate is proportional to the change in $\tan \delta$ for the system, such that

$$P_{\text{abs}} \propto \frac{(T - T_0)}{t} \propto \tan \delta \propto C_0 \quad (7)$$

P_{abs} is proportional to the measured frequency shift in the VNA, as recorded in Table 2.

The TOP-Te heating rates (Figure 6) exhibit linear concentration dependence for heating with a slope of 0.6 in BS and 0.2 in SiC, consistent with Eqn. 5. Heating in the noble-metal-coated SiC is invariant with concentration. The observation of reactants heating in SiC and BS when a MW-transparent solvent is used is further confirmed by comparing the rate of heating for TOP-Te in toluene to



the concentration-dependent heating curve for TOP-Te in EG (Supporting Information, SF 11). In that case, the heating rate was invariant with TOP-Te concentration.

Designing a better MW reaction vessel. In considering the design of a reaction vessel, it is imperative to interrogate the power absorbed by the vessel, to ensure the MW energy is absorbed in the wall of the vessel, so that it acts as a thermal susceptor in a MW-synthetic experiment. The absorbed power can be translated into the effect on MW reaction rates. MW chemistry is still a thermodynamics problem, in which the reaction rate scales with temperature above some critical activation energy. In a MW reaction, the heating rate will depend on the ability of components to absorb the MW energy, which is understood by considering the probability of absorption increasing with increasing D_p , and with the thickness (x) of the material being irradiated.

$$P_{abs} \propto e^{-x/D_p} \quad (8)$$

The results of the study show definitively that SiC is an effective molecular susceptor but that it is not an effective MW screen, as the VNA results exhibit a frequency shift that is correlated with $\tan \delta$ of the internal solvent. The modeling results and experimental data demonstrate that, to effectively screen the impinging MW field, the SiC vessel must be noble metal plated. To achieve the same shielding effect in unaltered SiC, the wall thickness would have to be a minimum of 193.0 mm (five D_p).

Table 3: Thermal lag (ΔT_r) and heating rate (dT/dt) for four solvents in each of the three microwave vessels used in the experiments, as recorded by the ruby thermometer (internal).

	BS		SiC		Au/SiC	
	ΔT_r (s)	dT/dt ($^{\circ}\text{C/s}$)	ΔT_r (s)	dT/dt ($^{\circ}\text{C/s}$)	ΔT_r (s)	dT/dt ($^{\circ}\text{C/s}$)
Toluene	3	0.59	8	4.1	8	2.01
Acetonitrile	3	4.84	6	2.6	8	2.14
Ethanol	3	5.37	4	2.7	11	1.53
EG	3	6.18	3	2.6	17	0.86

Noble metal plating will not work for all reactions, particularly if the layer is chemical unstable under the reaction conditions or if the metal acts as a catalyst. For instance, if the reaction conditions are very acidic, basic, or involve chalcogenides (sulfur, selenium, and tellurium) the metal plating may leach. In such a case, the addition of a PTFE lining could be incorporated for these situations, therefore it should be noted that this research has not explored all possible contingencies. Finally, it is important to note that for most research, the use of SiC vessels represents an important breakthrough pioneered by Anton Paar, particularly in systems wherein MW absorptivity into the solvent is poor and a MW susceptor is desirable.

Conclusions

MW chemistry suffers from the failure of many researchers to consider the entire system's interaction with the impinging EM field. The study demonstrates the importance of considering the MW photon interaction with all components of the reaction system utilized in chemical synthesis through the correlation of theory and experiment. The ED simulations show that significant penetration of the MW field is observed in BS and SiC, the depth of which is dependent on $\tan \delta$ of the internal solvent. Adding a thin, reflective layer of gold to the inner walls (Au/SiC) blocks MW radiation from interacting with the solvent. The results of the ED simulations are experimentally confirmed by VNA resonant frequency measurements. In the VNA studies, dramatic shifts in resonant frequency and FWHM of the cavity were observed. Insertion of the empty vessel results in an observable frequency shift. In the BS and SiC vessels, the observed resonant frequency shift and FWHM broadening is dependent on $\tan \delta$. The magnitude of shift and broadening was smaller in the SiC MW vessel than for the BS vessel. In the Au/SiC vessel, addition of solvent to the vessel caused no measurable subsequent shift. Additional confirmation of the effects of MW penetration was achieved by examining solutions of increasing molarity of TOP-Te in BS, SiC, and Au/SiC tubes, as a mimic for a chemical precursor initiated nanocrystal nucleation reaction. In the BS tube, a noticeable shift with increasing TOP-Te was recorded, and a similar but smaller shift was recorded in the SiC vessel. In the Au/SiC tube, however, the VNA resonant frequency was insensitive to TOP-Te concentration. The ED simulation, solvent VNA, and TOP-Se VNA results confirm the penetration depth of the MW is BS > SiC >>> Au/SiC.

The potential impact of MW penetration on chemical reactions is demonstrated by comparing the heating rates of four solvents heated in the three vessels in an Anton Paar MW unit. In the BS vessel, the heating rates increased with increasing $\tan \delta$ of the solvent; a similar trend was seen in the SiC vessel, attenuated by SiC's competitive absorption of MW energy. In contrast, heating curves of

solvents in the Au/SiC vessel followed the thermal diffusivities of the solvents, and not their $\tan \delta$ s. Solutions of increasing molarities of TOP-Te in toluene showed a distinct linear increase in heating rate in the BS, a less dramatic, but still linear heating rate in the SiC, and no effect of concentration of TOP-Te in the Au/SiC. The heating rate was also constant in the BS for increasing concentrations of TOP-Te in the MW-absorbing solvent EG, as predicted for the stronger MW absorptivity of EG. The results consistently demonstrate that the SiC tube is not completely shielding the contents from the MW field, and that a plating of a noble metal, such as gold, shields the contents from the radiation. These results suggest that conclusions about reaction mechanisms based upon the assumption that SiC absorbs all of the MW photons should be reconsidered when concluding rate enhancement effects in MW heating and conventional heating.

The observation that part-per-thousand concentrations of a strongly MW-absorbing reactant such as TOP-Te in a non-absorbing solvent can influence the heating rate has important implications for MW-controlled nanocrystal growth from molecular precursors dissolved in non-MW absorbing solvents. Whereas MW susceptors, highly absorbing vessels, and solvents enhance MW photon absorption, thermal transfer is dependent on the solvents' thermal diffusivity. The ability to distinguish among direct MW interactions with molecules in solution, direct solvent heating, and efficient convective radiative transfer from a reaction vessel in a MW reactor is important in understanding how MW reactions may differ from classically thermodynamic processes.

Acknowledgements

The project was funded in part by an Oak Ridge Institute for Science and Technology fellowship and NSF under NSF-CHE 0911080.

Notes and references

- [1] T. Razzaq and C.O. Kappe. *Chem. Sus. Chem.*, **2008**, *1*, 123–132.
- [2] C.O. Kappe. *Angew. Chem. Int. Ed.* **2004**, *43*, 6250–84.
- [3] T. M. Barnard, N.E. Leadbeater, M.B. Boucher, L.M. Stencel, B.A. Wilhite. *Energy Fuels*, **2007**, *21*, 1777–1781.
- [4] J.D. Moseley and C.O. Kappe. *Green Chem.* **2011**, *13*, 794–806.
- [5] N. E. Leadbeater in *Microwave Heating as a Tool for Sustainable Chemistry*. (Ed. N.E. Leadbeater) Taylor and Francis Group, Boca Raton, FL. **2010** pp. 9–13.
- [6] A. L. Washington and G. Strouse. *Chem. Mater.*, **2009**, *21*, 2770–277612.
- [7] K. Kim, R. Oleksak, E. Hostetler, D. Peterson, P. Chandran, D. Schut, B. Paul, G. Herman, C. Chang. *Cryst. Growth Des.* **2014**, *14*, 5349–5355.
- [8] M.B. Mohamed, K.M. Abouzeid, V. Abdelsayed, A.A. Aljarash, M.S. El-Shall. *ACS Nano.*, **2010**, *4*, 2766–2772.
- [9] T.M. Atkins, A. Thibert, D.S. Larsen, S. Dey, N. D. Browning, S. M. Kauzlarich. *J. Am. Chem. Soc.*, **2011**, *133*, 20664–20667.
- [10] J.A. Gerbec, D. Magana, A. Washington, G.F. Strouse. *J. Am. Chem. Soc.*, **2005**, *127*, 15791–15800.
- [11] D. Lovingood, J. Owens, M. Seeber, K. Kornev, and I. Luzinov. *ACS Appl. Mater. Interfaces.* **2012**, *4*, 6875–6883.
- [12] R. A. Hayn, J.R. Owens, S.A. Boyer, R. S. McDonald, H.J. Lee. *J. Mat. Sci.* **2011**, *46*, 2503–2509.
- [13] D. Lovingood, R. Oyler, G. Strouse. *J. A. m Chem. Soc.* **2008**, *130*, 17004–17011.
- [14] C.O. Kappe, B. Pieber, D. Dallinger. *Angew. Chem. Int. Ed.*, **2013**, *52*, 1088–1094.
- [15] B. Adnadjevic, J. Javanovic, B. Potkonjak. *Rus. J. of Phy. Chem. A.* **2013**, *87*, 2115–2120.
- [16] J. Binner, N. Hassine, T. Cross. *J. of Mat. Sci.* **1995**, *30*, 5389–5393
- [17] D. Steurga and P. Gaillard. *J.M.P.E.E.*, **1996**, *31*, 87–113.
- [18] A susceptor is considered any highly MW absorbing material added to the reaction system to enhance heating rates, such as ionic liquids, SiC, or carbon inserts; but that is not a catalyst nor is consumed in the chemical reaction.
- [19] A. de la Hoz, A. Diaz-Ortiz, A. Moreno. *Chem. Soc. Rev.*, **2005**, *34*, 164–178,
- [20] A. de la Hoz, A. Diaz-Ortiz, A. Moreno. *J.M.P.E.E.*, **2007**, *41*, 36–57.
- [21] M. Hosseini, N. Stiasni, V. Barbieri, C. Kappe, *J. Org. Chem.*, **2007**, *72*, pp 1417–1424
- [22] A. M. Rodriquez, P. Prieto, A. de la Hoz, A. Diaz-Ortiz, J.I. Garcia. *Org. Biomol. Chem.*, **2014**, *12*, 2436–2445.
- [23] G.B. Dudley, R. Richert, A.E. Stiegman. *Chem. Sci.* **2015**, *6*, 2144–2152.
- [24] a) M. Rosana, Y. Tao, A. Stiegman, G. Dudley. *Chem. Sci.*, **2012**, *3*, 1240–1244.
- [25] C.O. Kappe, B. Pieber, D. Dallinger. *Angew. Chem. Int. Ed.*, **2013**, *52*, 1088–1094
- [26] G.B. Dudley, A.E. Stiegman, M.R. Rosana. *Angew. Chem. Int. Ed.*, **2013**, *52*, 7918–7923
- [27] J. Hunt, A. Ferrari, A. Lita, M. Crosswhite, B.A. Ashley, A.E. Stiegman. *J. of Phys. Chem C.* **2013**, *117*, 26871–26880.
- [28] M. Crosswhite, J. Hunt, T. A. Southworth, K. Serniak, A. Ferrari, A.E. Stiegman. *ACS Catal.* **2013**, *3*, 1328–1323.
- [29] M.R. Rosana, J. Hunt, A. Ferrari, T.A. Southworth, Y. Tao, A. E. Stiegman, G.B. Dudley. *J. Org. Chem.* **2014**, *79*, 7437–7450.
- [30] A. M. Rodriquez, P. Prieto, A. de la Hoz, A. Diaz-Ortiz, J.I. Garcia. *Chemistry Open*, **2015**, online preview. <http://onlinelibrary.wiley.com/doi/10.1002/open.201402123/full>
- [31] N.E. Leadbeater and R.J. Smith. *Org. and Biomol. Chem.*, **2007**, *5*, 2770–2774.
- [32] a) J. Robinson, S. Kingman, D. Irvine, P. Licence, A. Smith, G. Dimitrakis, D. Obermayer, C. Kappe. *Phys. Chem. Chem. Phys.*, **2010**, *12*, 10793–10800.
- [33] B. Gutmann, D. Obermayer, B. Reichart, B. Prekodravac, M. Irfan, J. Kremsner, C. Kappe. *Chem. Eur. J.* **2010**, *16*, 12182–12194.
- [34] W. Huang and R. Richert. *J. Phys. Chem. B.* **2008**, *112*, 9909–9913.
- [35] W. Huang and R. Richert. *J. Chem. Phys.* **2009**, *130*, 194509.
- [36] M. B. Gawande, S. N. Shelke, R. Zboril, R. S. Varma. *Acc. Chem. Res.*, **2014**, *47*, 1338 – 1348.
- [37] A. K. Rathi, M. B. Gawande, R. Zboril, R. S. Varma. *Coor. Chem. Rev.*, **2015**, *291*, 68 – 94.
- [38] J. Baker-Jarvis, E. Vanzura, W. Kissick, *IEEE Trans. Microwave Theory Tech.* **1990**, *38*, 1096–1103.
- [39] Personal email correspondence with Anton Paar representative R. Klopfer, March 20-23, 2015. The cavity is TE_{10x} with x = 1 nominally, but depending on reaction conditions x may be equal to 2, 3, etc.
- [40] W.E. Benet, G.S. Lewis, L.Z. Yang, P.D.E. Hughes. *J. Chem. Res.* **2011**, *35*, 675–677.
- [41] E.H. Williams, A.V. Davydov, A. Motayed, S.G. Sundaresan, P. Bocchini, L.J. Richter, G.Stan, K Steffens, R. Zangmeister, J. Schreifels, M.V. Rao. *App. Surf. Sci.* **2012**, *258*, 6056–6063.
- [42] A.C. Metaxas and R. J. Meredith. *Industrial Microwave Heating*. 1st ed. The Institution of Engineering and Technology. **2008**. pp 5–24
- [43] A.C. Metaxas and R. J. Meredith. *Industrial Microwave Heating*. 1st ed. The Institution of Engineering and Technology. **2008**. pp 70–102
- [44] A. von Hippel in *Dielectric Materials and Applications*. (ed. A. von Hippel) Artech House, Boston, London. **1995**. pp. 30–37
- [45] A.F. Harvey. *Microwave Engineering*. Academic Press, New York, **1963**. p. 251.
- [46] D.M. Pozar. *Microwave Engineering*. John Wiley & Sons, Inc. 3rd ed. **2005**. p. 687
- [47] B.L. Hayes. *Microwave Chemistry: Chemistry at the Speed of Light*. CEM Corp. 1st ed. **2002** p. 35

[48] D. Lide, editor-in-chief. *CRC Handbook of Chemistry and Physics*. CRC Press. 85th ed. **2004**

[49] J. C. Slater. *Reviews of Modern Physics*. **1946**, *18*, 441–512.

[50] D. Obermayer, B. Gutmann, C.O. Kappe. *Angew. Chem. Int. Ed.* **2009**, *121*, 8471–8474.

[51] A.C. Metaxas and R. J. Meredith. *Industrial Microwave Heating*. 1st ed. The Institution of Engineering and Technology. **2008**. pp 48–53.

[52] J. D. Piper in *Dielectric Materials and Applications*. (ed. A. von Hippel) Artech House, Boston, London. **1995**. p. 158.